

TOWARDS REDUCING THRUSTER- FLEXIBILITY INTERACTIONS IN SPACE ROBOTS

E. Martin E. Papadopoulos J. Angeles

Department of Mechanical Engineering & Centre for Intelligent Machines,
McGill University, Montreal, Quebec, Canada, H3A 2K6

Abstract

Space manipulators mounted on an on-off thruster-controlled base are envisioned to assist in the assembly and maintenance of space structures. When handling large payloads, manipulator joint and link flexibility become important, for they can result in payload-attitude controller fuel-replenishing dynamic interactions. In this paper, the dynamic behavior of a flexible-joint manipulator on a free-flying base is approximated by a single-mode mechanical system, while its parameters are matched with space-manipulator data. Describing functions are used to predict the dynamic performance of three alternative controller-estimator schemes, and to conduct a parametric study on the influence of key system parameters. Design guidelines and a state-estimator are suggested that can minimize such undesirable dynamic interactions as well as thruster fuel consumption.

Introduction

Robotic devices in orbit will play an important role in space exploration and exploitation. The mobility of such devices can be enhanced by mounting them on free-flying bases, controlled by on-off thrusters. Such robots introduce a host of dynamic and control problems not found in terrestrial applications. When handling large payloads, manipulator joint or structural flexibility becomes important and can result in payload-attitude controller fuel-replenishing dynamic interactions. Such interactions may lead to control system instabilities, or manifest themselves as limit cycles¹.

The CANADARM-Space Shuttle system is the only operational space robotic system to date. Its Reaction Control System (RCS), which makes use of on-off thrusters, is designed assuming rigid body motion, and using single-axis, thruster switching logic based on phase-plane techniques. This approach is common in the design of thruster-based control systems. However, the flexible modes of this space robotic system have rather low frequencies, which continuously change with manipulator configuration and payload, and can be excited by the RCS activity. The performance degradation of the RCS due to the deployment of a flexible *payload*, with or without the CANADARM has been studied². A new design for the RCS was developed to reduce the impact of large measurement uncertainties in the rate signal during attitude control, thereby increasing significantly the performance of the RCS for rigid-body motion³. However, the flexibility problem was not addressed. Currently, the method for resolving these problems consists of performing extensive simulations. If dynamic interactions occur, corrective actions are taken, which

would include adjusting the RCS parameter values, or simply changing the operational procedures². The consequences of such interactions can be problematic, since fuel is an unavailable resource in space; hence, classical attitude controllers must be improved to reduce the possibility of such dynamic interactions.

This problem was studied using a single-mode, linear translational mechanical system to approximate the dynamic behavior of a two-flexible-joint manipulator mounted on a three-degree-of-freedom (dof) base⁴. A state-estimator and design guidelines were suggested to minimize such undesirable dynamic interactions, as well as thruster fuel consumption. In that study, the damping ratio of the system was taken constant and equal to 0.05. However, the damping ratio will in general be a function of the manipulator configuration and its payload. This paper reports results obtained under these more realistic conditions. In Section 2, the required damping ratios for all configurations and payloads are obtained using the dynamics model of a two-dof planar manipulator mounted on a three-dof spacecraft. The control laws and models used are then derived in Section 3. Finally, in Section 4, the describing-function method and simulations are used to study this approximate system, and show the improved performance that can be obtained using the state-estimator model previously developed⁴. Design guidelines are also given.

Modeling

The dynamics model of the two-flexible-joint planar manipulator mounted on a free-floating base of Fig. 1(a), was developed using a Lagrangian formulation under the assumption that all link and joint flexibilities are lumped at the joints⁵. This is reasonable, since joint flexibility is more significant than link flexibility in this kind of system. Each flexible joint is modeled as a torsional spring in parallel with a torsional dashpot. Using linearization techniques and a proper change of variables, the system reduces to two decoupled equations describing the joint flexibility modes, and two equations giving the torque required to brake the joints in a specific configuration. In order to obtain these two decoupled equations, the damping at the joints is assumed proportional to the respective stiffness of these joints, thereby obtaining

$$\ddot{y}_i + \lambda\omega_i^2\dot{y}_i + \omega_i^2y_i = 0, \quad i = 1, 2 \quad (1)$$

where λ is the proportionality constant and ω_i is the natural frequency, that can be readily derived⁵. Comparing Eq. (1) to the standard second-order form,

$$\ddot{y}_i + 2\zeta_i\omega_i\dot{y}_i + \omega_i^2y_i = 0, \quad i = 1, 2 \quad (2)$$

we have

$$2\zeta_i\omega_i = \lambda\omega_i^2, \quad i = 1, 2 \quad (3)$$

which implies that $\zeta_2 = \zeta_1(\omega_2/\omega_1)$.

Thus, if $\omega_2 > \omega_1$, we must have $\zeta_2 > \zeta_1$ in order to have proportional damping. This is in agreement with published data for the CANADARM/Space Shuttle system, where it can be observed that the oscillations corresponding to the second and higher modes die out very quickly, and thus, the first mode dominates the response of the system⁶. Therefore, the hypothesis of proportional damping is reasonable.

Considering that two different joints are used, the approximate characteristics of the CANADARM/Space Shuttle system are used together with the frequency expressions

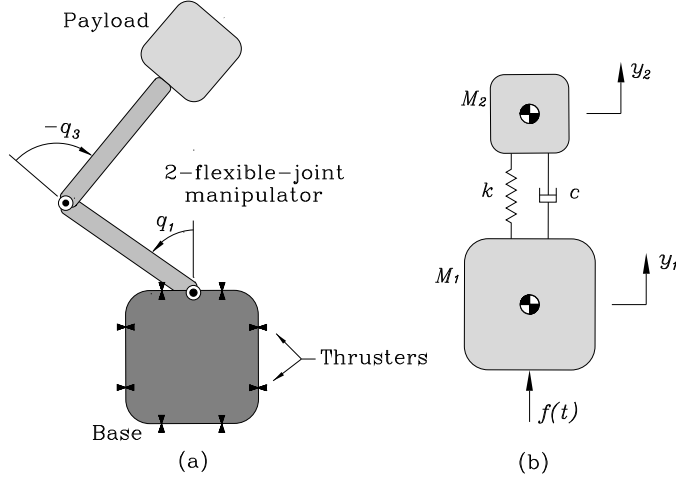


Figure 1: Flexible manipulator replaced by a spring and a dashpot: (a) two-link manipulator on a floating base; (b) simplified two-mass system.

ω_i to obtain the first natural frequency and the damping ratio of this system for many configurations and payloads. The results are recorded in Tables 1 and 2 for $q_1 = 45^\circ$, where β is defined as the ratio of the mass of the payload over the mass of the base. In these two tables, varying the payload from 0 to 30% of the spacecraft result in a 12-fold change in natural frequency and damping ratio.

Table 1: First natural frequency evaluation for $q_1 = 45^\circ$ (ω_1) (Hz).

β	$q_3 = -135^\circ$	$q_3 = -90^\circ$	$q_3 = -45^\circ$	$q_3 = 0^\circ$
0.	0.653	0.429	0.343	0.320
0.01	0.254	0.170	0.137	0.128
0.05	0.127	0.091	0.077	0.073
0.1	0.095	0.073	0.064	0.062
0.15	0.082	0.066	0.059	0.057
0.2	0.074	0.062	0.057	0.055
0.25	0.069	0.059	0.055	0.053
0.3	0.065	0.057	0.054	0.052

Table 2: Damping ratio evaluation for $q_1 = 45^\circ$ (ζ_1).

β	$q_3 = -135^\circ$	$q_3 = -90^\circ$	$q_3 = -45^\circ$	$q_3 = 0^\circ$
0.	0.102	0.067	0.054	0.050
0.01	0.040	0.027	0.021	0.020
0.05	0.020	0.014	0.012	0.011
0.1	0.015	0.011	0.010	0.010
0.15	0.013	0.010	0.009	0.009
0.2	0.012	0.010	0.009	0.009
0.25	0.011	0.009	0.009	0.008
0.3	0.010	0.009	0.008	0.008

The dynamics of a simple two-flexible-joint planar manipulator is rather complicated; it is preferable to employ a simplified model to analyze the problem stated in the previous

section. We can replace the manipulator of Fig. 1(a) with an equivalent two-mass-spring-dashpot system, as shown in Fig. 1(b). By a proper selection of the spring stiffness k and the damping coefficient c , the resonant frequency of the simplified system can be matched to the lowest one of the original system. Therefore, a similar relative motion of the payload with respect to the base can be obtained. The derivation of the equations of motion for this simplified system is straightforward and is skipped here^{4,5}.

Control

Control Schemes

Currently available technology does not allow the use of proportional thruster valves in space, and thus, the classical PD and PID control schemes cannot be used. Therefore, spacecraft attitude and position are controlled by the use of on-off thruster valves, that introduce nonlinearities.

The usual scheme to control a spacecraft with on-off thrusters is based on the error phase plane, defined as that with spacecraft attitude error e and error-rate \dot{e} as coordinates. The on-and-off switching is determined by switching lines in the phase plane and can become complex, as is the case in the phase plane controller of the Space Shuttle². To simplify the switching logic, two switching lines with equations $e + \lambda\dot{e} = \pm\delta$ have been used. The deadband limits $[-\delta, \delta]$ are determined by attitude limit requirements, while the slope of the switching lines, by the desired rate of convergence towards equilibrium and by the rate limits. This switching logic can be represented as a relay with a deadband, where the input is $e + \lambda\dot{e}$, the left-hand side of the switching-line equations⁴.

To compute the input to the controller, the position and the velocity of the system base are required. Using current space technology, both states can be obtained by sensor readings. However, it can happen that only the attitude is available and then, the velocity must be estimated. In this paper, three models previously studied are considered⁴. For the first model, Case 1, both the position and the velocity of the base are available by sensors and these signals are simply passed through filters to eliminate high-frequency noise. For the other two models, we assume that only the position is available from sensors and state estimators are used to obtain the required velocity. In Case 2, we differentiate the position signal while passing it through a filter to obtain an estimate for the velocity. The position signal is also filtered in this case. Finally, for the model corresponding to Case 3, a classical asymptotic state observer is used to obtain an estimate for the position and the velocity.

In all three cases, a time delay τ has been included to account for the delay between the time a sensor reads a measurement, and the time this measurement is used. Since this delay is more significant than the delay of turning on or off the thrusters, only a sensor time delay is included.

Frequency-Domain Analysis

The attitude controller assumes on-off thrusters, which are nonlinear devices; hence, the system cannot be adequately analyzed through the application of linear analysis methods. This problem is addressed using the describing-function method, which can predict the existence of limit cycles in nonlinear systems^{7,8}.

In order to use this method, the system under study must be partitioned into a linear and a nonlinear part. Then, the system is transformed into the configuration shown in Fig. 2, whereby $G(j\omega)$ is the frequency response of all the linear elements in the system and $N(A, \omega)$ is the describing function of the nonlinearity, which is tabulated in books⁸. For the three cases mentioned in the previous subsection, it is always possible to reduce the block diagrams in the configuration of Fig. 2. A detailed description of this method can be found in the literature^{7,8}. The application of the method to the problem at hand, along with the stability definition used in this paper, are reported elsewhere⁴.

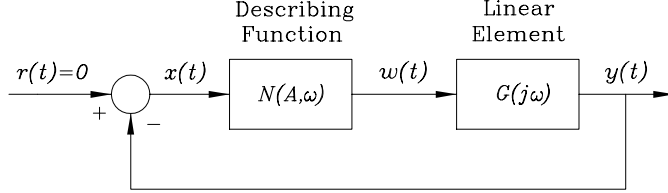


Figure 2: A feedback system whose nonlinear part has been replaced by its corresponding describing function.

Parametric Studies and Results

Using the describing function method, a parametric study was undertaken to investigate the significance of key system parameters. The three cases discussed in Section 3 are analyzed using the fixed parameter values of Table 3, and the range of parameter values of Table 4, both being based on available space manipulator data⁵.

Table 3: Fixed-parameter values.

q_1	τ (s)	ω_{se} (rad/s)	ζ_f	ζ_{se}
45°	0.1	0.2513	0.707	0.707

Table 4: Free-parameter values.

β	$0.01 \leq \beta \leq 0.3$
λ (s)	$0.1 \leq \lambda \leq 50$
a_0 (m/s ²)	$0.0002 \leq a_0 \leq 0.02$
δ (m)	$0.001 \leq \delta \leq 0.1$
q_3	$-135^\circ, -90^\circ, -45^\circ, 0^\circ$
ω_f (rad/s)	$0.2513 \leq \omega_f \leq 5$

The results of the parametric study for Case 2 are illustrated with the use of stability maps, as depicted in Fig. 3. Figure 3(a) shows the stability boundary for different cutoff frequencies ω_f of the employed second-order filter. The region below such boundary represents a zone where the system is stable, while the region above corresponds to a zone of instability. As shown in the same figure, the stability zone can be increased by increasing the cutoff frequency ω_f . A similar analysis of the graphs of Fig. 3 leads to guidelines for the design of attitude control systems when flexibility is a major concern, namely,

1. The cutoff frequency ω_f for the filters should be chosen as large as possible to avoid instability.
2. The velocity gain λ should be chosen as large as possible to avoid instability.
3. The acceleration of the base a_0 should be kept small for stability. Unstable types of behavior are more likely to occur for large a_0 .
4. Deadband limits δ should be chosen as large as possible to avoid instability.

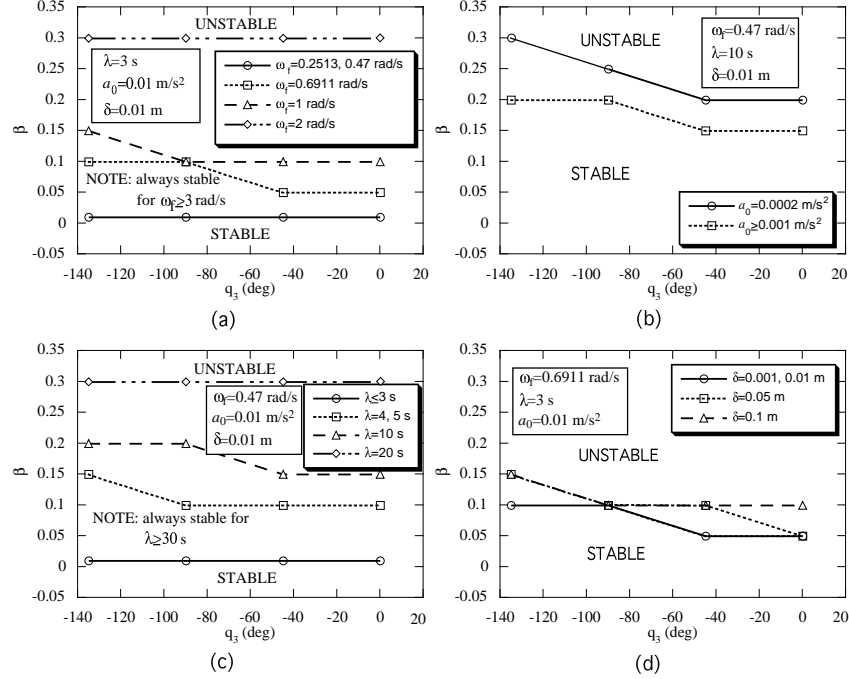


Figure 3: Describing function stability maps for Case 2 showing: (a) the effect of the cutoff frequency ω_f ; (b) the effect of the base acceleration a_0 ; (c) the effect of the velocity gain λ ; and (d) the effect of the deadband limit δ .

The upper limits of these parameters are set by design requirements or available hardware.

The same conclusions are drawn when Case 1 is analyzed. However, in general, the performance of Case 1 is worse than that for Case 2. To demonstrate this, the system configuration for Case 1 with parameters given in Tables 3 and 5 was used. Simulation results, for an initial error of 0.05 m, are shown in Fig. 4. Figures 4(b) and (c) show that thrusters are firing continuously, thus resulting in a high total fuel consumption of 491.1 fuel units, and a large rate of fuel consumption. Therefore, the system is classified as unstable. Moreover, the phase-plane trajectories of Fig. 4(a) show that a large limit cycle is reached due to the dynamic interactions.

If the model of Case 2 is simulated with the same parameter values, the results of Fig. 5 are obtained. Examining Figs. 5(b) and (c), we observe that thrusters are firing continuously, and that the total fuel consumption is quite high, namely, 430.8 fuel units. Therefore, this system is also considered unstable. The same conclusion is reached with the describing function method, as illustrated in Fig. 3(c) for $\lambda = 3$ s. Thus, the results corresponding to Cases 1 and 2 are both unstable, but the performance of Case 1 is worse than that for Case 2, since the fuel consumption is higher.

On the other hand, using the system configuration of Case 3, with the same parameters,

Table 5: Free-parameter values used for simulations.

β	λ (s)	a_0 (m/s^2)	δ (m)	ω_n (rad/s)	ζ	ω_f (rad/s)
.3	3	0.01	0.01	$2\pi(0.052)$	0.008	0.47

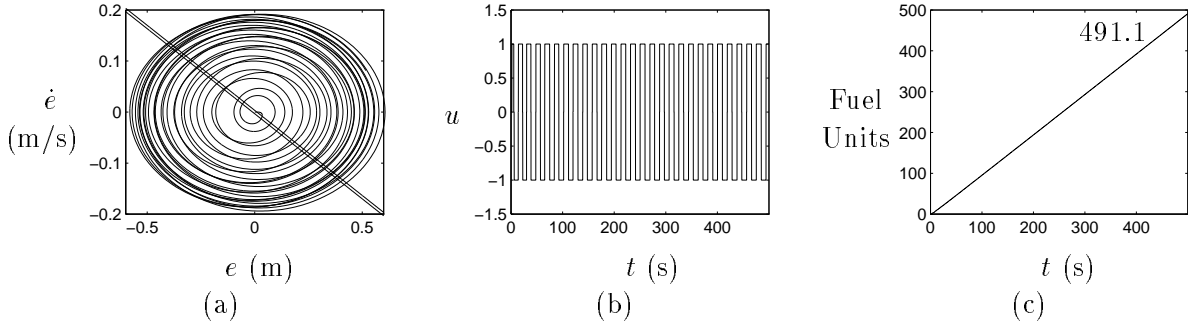


Figure 4: Simulation results using the Case 1 model: (a) Spacecraft error phase plane; (b) Thruster command history; and (c) Fuel consumption.

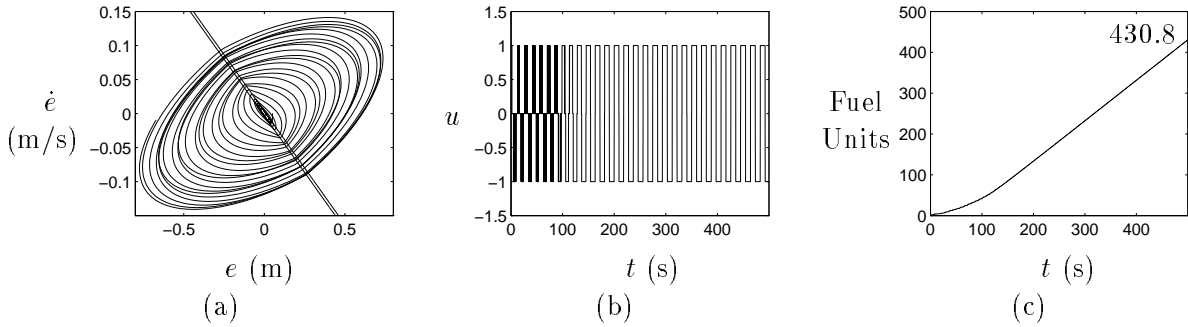


Figure 5: Simulation results using the Case 2 model: (a) Spacecraft error phase plane; (b) Thruster command history; and (c) Fuel consumption.

provides very interesting results, as shown in Fig. 6. From Fig. 6(a), it can be seen that a limit cycle contained between the switching lines is reached, which results in a stable system. One can note a spiral motion due to the relative motion between the two masses, that damps out. Figures. 6(b) and (c) are also typical of a stable system, since the thrusters are not firing continuously and the fuel-consumption curve is flat, thereby resulting in a near-zero rate of fuel consumption, similar to that for a rigid body system. In this case, the total fuel consumption is very small, namely, 7.2 fuel units only. Therefore, it is observed that the use of the proposed state estimator increases the performance of the control system significantly, and extends the operational life of the system. In addition, using the describing function method, it can be shown that this estimator results in a system that is almost always stable for the whole range of parameters, thus resulting in significantly increased stability margins in comparison to Cases 1 and 2. Using simulation, it was shown that the performance of this estimator remains very good in the presence of noise and model uncertainties⁵.

Conclusions

This paper reports describing function results when the damping ratio is assumed to vary with the configuration of the manipulator and its payload. These results are almost the same as those obtained using a constant damping ratio of 0.05⁴. In fact, the general trends, or guidelines, are the same, but the particular values are different. Many configurations that were previously ascertained as stable are now found to be unstable. This more accurate analysis shows that the domain of instability is larger than previously thought.

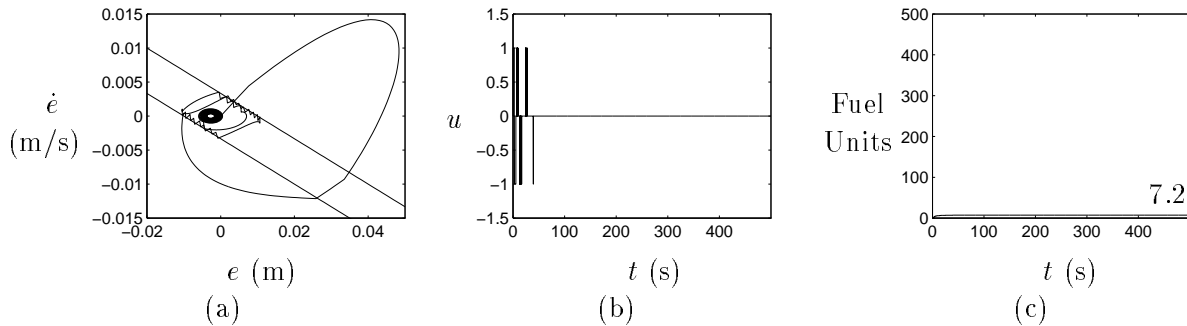


Figure 6: Simulation results using the Case 3 model: (a) Spacecraft error phase plane; (b) Thruster command history; and (c) Fuel consumption.

This makes the development of control methods aiming at improving performance more important and challenging.

Acknowledgements

The support of this work by the Fonds pour la Formation de Chercheurs et l'Aide à la Recherche (FCAR) and by the Natural Sciences and Engineering Council of Canada (NSERC) is gratefully acknowledged. The first author is an NSERC Class-of-67 Scholar.

REFERENCES

- [1] Millar, R. A., and Vigneron, F. R., "Attitude Stability of a Pseudorate Jet-Controlled Flexible Spacecraft," *J. of Guid., Cont., and Dyn.*, Vol. 2, No. 2, 1979, pp. 111–118.
- [2] Sackett, L. L., and Kirchwey, C. B., "Dynamic Interaction of the Shuttle On-Orbit Flight Control System with Deployed Flexible Payload," *Proc. of the AIAA Guid. and Cont. Conf.*, San Diego, CA, 1982, pp. 232–245.
- [3] Kubiak, E. T., and Martin, M. W., "Minimum Impulse Limit Cycle Design to Compensate for Measurement Uncertainties," *J. of Guid., Cont., and Dyn.*, Vol. 6, No. 6, 1983, pp. 432–435.
- [4] Martin, E., Papadopoulos, E., and Angeles, J., "On the Interaction of Flexible Modes and On-off Thrusters in Space Robotic Systems," *Proc. of the 1995 Int. Conf. on Intelligent Robots and Systems, IROS'95*, Vol. 2, Pittsburgh, PA, 1995, pp. 65–70.
- [5] Martin, E., "Interaction of Payload and Attitude Controller in Space Robotic Systems," Master Thesis, Dept. of Mech. Eng., McGill University, Montreal, Canada, 1994.
- [6] Singer, N. C., "Residual Vibration Reduction in Computer Controlled Machines," Technical Report 1030, MIT Artificial Intelligence Laboratory, Cambridge, MA, 1989.
- [7] Slotine, J.-J. E., and Li, W., *Applied Nonlinear Control*, Prentice Hall, Englewood Cliffs, N.J., 1991.
- [8] Atherton, D. P., *Nonlinear Control Engineering*, Van Nostrand, New York, 1975.